haematologica
Journal of the Ferrata Storti Foundation

Myeloma cell growth suppression by osteoblast-derived extracellular vesicles: the creation of a non-permissive niche for myeloma cells by bone-forming osteoblasts

by SooHa Kim, Jumpei Teramachi, Masahiro Hiasa, Ryota Amachi, Ariunzaya Bat-Erdene, Asuka Oda, Hirofumi Tenshin, Mariko Tanaka, Motosumi Nakagawa, Aiko Seki, Yoshihiko Sawa, Ken-ichi Matsuoka, Eiji Tanaka, Takeshi Harada, Tatsuya Tominaga, and Masahiro Abe

Received: September 3, 2024.
Accepted: January 10, 2025.

Citation: SooHa Kim, Jumpei Teramachi, Masahiro Hiasa, Ryota Amachi, Ariunzaya Bat-Erdene, Asuka Oda, Hirofumi Tenshin, Mariko Tanaka, Motosumi Nakagawa, Aiko Seki, Yoshihiko Sawa, Ken-ichi Matsuoka, Eiji Tanaka, Takeshi Harada, Tatsuya Tominaga, and Masahiro Abe. Myeloma cell growth suppression by osteoblast-derived extracellular vesicles: the creation of a non-permissive niche for myeloma cells by bone-forming osteoblasts. Haematologica. 2025 Jan 23. doi: 10.3324/haematol.2024.286554 [Epub ahead of print]

Myeloma cell growth suppression by osteoblast-derived extracellular vesicles: the creation of a non-permissive niche for myeloma cells by bone-forming osteoblasts

SooHa Kim[1,2], Jumpei Teramachi[3], Masahiro Hiasa[1], Ryota Amachi[1], Ariunzaya Bat-Erdene[4,5], Asuka Oda[2], Hirofumi Tenshin[1], Mariko Tanaka[1, 2], Motosumi Nakagawa[1, 2], Aiko Seki[3], Yoshihiko Sawa[3], Ken-ichi Matsuoka[2], Eiji Tanaka[1], Takeshi Harada[2], Tatsuya Tominaga[6] and Masahiro Abe[7]

[1]Department of Orthodontics and Dentofacial Orthopedics, Tokushima University Graduate School of Biomedical Sciences, Tokushima, Japan; [2]Department of Hematology, Endocrinology and Metabolism, Tokushima University Graduate School of Biomedical Sciences, Tokushima, Japan; [3]Department of Oral Function and Anatomy, Graduate School of Medicine Dentistry and Pharmaceutical Sciences, Okayama University, Japan; [4]Department of Immunology, School of Bio-Medicine, Mongolian National University of Medical Sciences, Ulaanbaatar, Mongolia; [5]Department of Health Research, Graduate School of Mongolian National University of Medical Sciences, Ulaanbaatar, Mongolia; [6]Department of Bioanalytical Technology, Tokushima University Graduate School of Medical Sciences, Tokushima, Japan and [7]Department of Hematology, Kawashima Hospital, Tokushima, Japan

Corresponding authors: Jumpei Teramachi, Department of Oral Function and Anatomy, Graduate School of Medicine Dentistry and Pharmaceutical Sciences, Okayama University, 2-5-1 Shikata-cho, Kita-ku, Okayama, 700-8525 Japan, TEL: +81-86-235-6636, e-mail: jumptera@okayama-u.ac.jp; Masahiro Abe, Department of Hematology, Kawashima Hospital, 6-1 Kitasako-ichibancho, Tokushima, 770-0011 Japan, TEL: +81-88-631-0110, e-mail: masabe@tokushima-u.ac.jp

Funding: This work was supported in part by the JSPS KAKENHI Grant Numbers; JP24K02643, JP22K19626, JP21H03111, JP23K27791, JP24K22250, JP22K08455 and the Research Clusters program of Tokushima University. The funders had no role in study design, data collection and analysis, decision to publish, or preparation of the manuscript.

Competing Interests: M.A. received research funding from Chugai Pharmaceutical, Sanofi K.K., Pfizer Seiyaku K.K., Kyowa Hakko Kirin, MSD K.K., Astellas Pharma, Takeda Pharmaceutical, Teijin Pharma and Ono Pharmaceutical, and honoraria from Daiichi Sankyo Company. Other authors declare no competing financial interests.

Data-sharing statement:

The corresponding authors are available to share any requested original data and protocols with other investigators upon reasonable request.

Author Contributions:

SH.K., J.T. and M.A. designed the research and conceived the project; isolation of EVs and PCR was performed by SH.K., J.T., T.H. and T.T.; flow cytometry by SH.K., M.H., A.O. and T.H.; immunoblotting by SH.K., J.T, R.A. A.BE., and H.T.; EV transfer assay by SH.K., J.T., A.S. and Y.S.; cell cultures by SH.K., J.T. M.H., R.A., A.BE., A.O., H.T., M.T. and T.H.; data analysis by SH.K., J.T. M.H., R.A., A.BE., A.O., H.T., KI.M., E.T., T.H., T.T. and M.A.; J.T. and M.A. wrote the manuscript.

Multiple myeloma (MM) cells are generally accepted to preferentially grow in the bone marrow niche, where bone marrow stromal cells (BMSCs) play a central role. BMSCs are osteoblast (OB) precursor cells, and their differentiation into bone-forming, mature OBs is inhibited by various factors in MM. In sharp contrast to BMSCs, terminally differentiated OBs actively producing bone matrices have been demonstrated to induce apoptosis in MM cells but not in normal hematopoietic cells [1-3]. However, the precise mechanisms for MM cell growth suppression by bone-forming, mature OBs remain largely unknown. We demonstrate here that the expression of microRNA (miR)-125b, a tumor suppressor gene for MM cells, is repressed in MM cells but upregulated in mature OBs actively producing bone matrix, and OB-derived miR125-b is transferred via extracellular vesicles (EVs) into MM cells, causing MM cell death in parallel with reductions in interferon regulatory factor 4 (IRF4) and MYC expression levels. These results suggest the importance of bone health with bone formation in MM treatment and therapeutic opportunities with synthetic miR-125b mimics.

MM has the unique propensity to develop and expand almost exclusively in bone marrow, resulting in bone destruction. MM cells enhance osteoclastogenesis while suppressing osteoblastogenesis, leading to devastating bone destruction with rapid loss of bone. MM cell-induced cell types in MM bone lesions, namely osteoclasts (OCs), vascular endothelial cells and BMSCs with defective osteoblastic differentiation, play an important role in creating a cellular microenvironment suited for MM cell growth and survival as feeders for MM cells. Intriguingly, tumor regression has been demonstrated to occur within bone along with inducing bone formation in MM animal models treated with bone-anabolic agents, such as an anti-DKK1 antibody [4], lithium chloride [5], and TGF-β inhibitor [2] although these agents alone did not impair MM growth *in vitro*. These findings suggest a correlation between the pharmacological induction of active bone formation and tumor regression in bone. Consistent with these *in vivo* observations, we and others reported that terminally differentiated OBs actively producing bone matrices induced apoptosis in MM cells but not in normal hematopoietic cells, whereas BMSCs, OB precursor cells, enhanced MM cell growth and viability [1-3]. Importantly, the suppressive activity of MM cell growth was produced exclusively by terminally differentiated OBs with mineralized nodule formation, while OBs at earlier differentiation stages with increased alkaline activity without mineralized nodule formation did not reduce the growth and viability of MM cells [2]. However, the precise underlying mechanisms for MM cell growth suppression by terminally differentiated, bone-forming OBs remain largely unknown.

IRF4 has been demonstrated to be a master transcription factor vital for MM cell growth and survival, and it is regarded as a therapeutic target specific for MM [6, 7]. IRF4 has been reported to be a target of miR-125b [8, 9]. Morelli, et al. reported that miR-125b expression was repressed in MM cells, especially in those residing in the bone marrow microenvironment,

and that enforced expression of miR-125b downregulated IRF4 and MYC expression in patient-derived MM cells and MM cell lines, and thereby suppressed MM cell growth [10]. In regard to miR-125b, OB-derived extracellular matrix vesicles have been demonstrated to be highly enriched with miR-125b [11]. There is a similarity between extracellular matrix vesicles and exosomes as EVs in terms of containing miRs. In the present study, we explored the mechanisms of MM cell growth inhibition by terminally differentiated, bone-forming OBs with special reference to OB-derived EVs.

Consistent with the previous observations [1-3], the viability of MM cell lines (Figure 1A and Supplementary Figure 1A, B) and primary MM cells (Supplementary Figure 1C) was reduced over time in cocultures with mature OBs with mineralized nodule formation differentiated from MC3T3-E1 preosteoblastic cells by BMP-2. However, MC3T3-E1 preosteoblastic cells without OB differentiation did not impair MM cell growth. Similar suppressive activity for MM cell lines was produced by mature OBs with mineralized nodule formation differentiated from IDG-SW3 osteoblastic cells (Figure 1B) and primary bone marrow stromal cells (Supplementary Figure 1D). In addition, the cocultures with mature OBs substantially reduced the protein levels of the vital survival factors IRF4 and MYC in MM cells (Figure 1C).

We next isolated EVs from supernatants of MC3T3-E1 and IDG-SW3-derived OBs with mineralized nodule formation and examined the effects of the isolated EVs on MM cell growth. Addition of mature OB-derived EVs induced cell death in MM cell lines and primary MM cells (Figure 2A). MM cells underwent apoptosis by the treatment with OB-derived EVs (Supplementary Figure 2A, B). To detect the incorporation of EVs, we labeled RNA in EVs isolated from mature OBs, and incubated the RNA-labeled EVs with MM cells. After 24 hours, the RNA-labeled EVs were detected in MM cells (Figure 2B). However, treatment with the EV uptake inhibitor Dynasore blocked incorporation of the RNA-labeled EVs, although not completely (Supplementary Figure 2C), and alleviated EV-induced MM death (Supplementary Figure 2D). Notably, the addition of mature OB-derived EVs did not affect the viability of different types of normal cells other than MM cells, including peripheral blood mononuclear cells, BMSCs, bone marrow macrophages, OCs, and OBs (Figure 2C). Therefore, OB-derived EVs are suggested to selectively kill MM cells but not other types of cells in the MM tumor micro-environment in the bone marrow.

Among others, miR-125b has been reported to be produced in OBs [11] and act as a tumor suppressor microRNA for MM cells [10]. The mouse and human miR-125b sequences share 100% homology. We next looked at the expression of miR-125b in terminally differentiated OBs with mineralized nodule formation, which can suppress MM cell growth. The expression of miR-125b was substantially upregulated in terminally differentiated OBs with mineralized

nodule formation derived from MC3T3-E1 and IDG-SW3 cells (Figure 3A). Consistent with the previous report [10], miR-125b was only marginally expressed in MM cell lines and primary MM cells compared with MC3T3-E1 cells (Figure 3B and Supplementary Figure 3A). Similar to its cellular expression, miR-125b levels were higher in EVs isolated from culture supernatants of mature OBs differentiated from MC3T3-E1 and IDG-SW3 cells than those from untreated MC3T3-E1 and IDG-SW3 cells, respectively (Figure 3C). miR-125b was marginally detected in EVs isolated from culture supernatants of OCs but not from MM cells. Notably, although MM cells cultured alone only marginally expressed miR-125b, miR-125b was detected in MM cells after coculturing with OBs forming mineralized nodules (Figure 3D). Similar to the effects of mature OBs (Figure 1C), the addition of OB-derived EVs decreased the protein levels of IRF4 and MYC in MM cells (Figure 3E), suggesting a role of OB-derived EVs in suppression of the IRF4-MYC axis in MM cells. However, transfection of a miR-125b inhibitor into MM cells suppressed MM cell death induced by OB-derived EVs (Figure 3F). These results suggested that miR-125b plays an important role in MM cell death induced by OB-derived EVs.

Together with the *in vivo* observations of MM tumor regression in a bone-forming milieu [1-5], the present study suggests that OBs with bone-forming activity might be a distinct cell type that creates a non-permissive niche for MM growth and survival in bone marrow. Proteasome inhibitors exert bone anabolic actions in bone lesions in responders to them; therefore, the expression of miR-125b in primary MM cells may be increased when bone formation is restored after treatment with proteasome inhibitors, although bortezomib treatment did not directly affect miR-125b expression in MM cells as well as osteoblasts *in vitro* (Supplementary Figure 3B). Alteration of miR-125b levels in primary MM cells during disease progression and their correlation with response to treatment should be clarified to elucidate MM biology in terms of MM cell-bone marrow interaction. Active OBs distinguishably produce a large amount of extracellular matrices; therefore, the role of extracellular matrix produced by active OBs has been studied in relation to the regression of MM growth. The small leucine-rich proteoglycan decorin is abundantly produced by mature OBs and its role in mature OB-mediated MM regression has been reported [12]. However, decorin alone did not induce apoptosis in MM cells as potently as mature OBs did in our experimental conditions [2]. Multiple factors produced by mature OBs may act together to impair MM cell growth and survival. The present study suggests that EV-mediated transfer of miR-125b from mature OBs into MM cells causes at least partial suppression of MM cell growth and survival, which contributes to the formation of an OB-mediated non-permissive niche for MM cells. OB-derived miR-125b has also been reported to suppress OC differentiation [11, 13], further suggesting the therapeutic roles of OB-derived EVs in the amelioration of bone disease together with MM tumor containment. Consistent with the previous study [10], we demonstrated that miR-125b suppresses the expression

of IRF4 and MYC to induce apoptosis in MM cells. miR-125b can inhibit translation through binding to the 3′ untranslated regions (3′-UTR) of various target mRNAs, and has been demonstrated to repress the expression of various important mediators for growth and survival signaling pathways, including NF-κB, PI3K/Akt/mTOR, ErbB2 and Wnts [14]. Therefore, EV transfer of miR-125b into MM cells may repress the expression of various genes responsible for MM cell growth, survival and function, which remains to be clarified. Delivery of isolated mature OB-derived EVs or engineered nano-particles containing synthetic miR-125b mimics may open an avenue to offer innovative therapeutic opportunities to treat MM.

References

1. Yaccoby S, Wezeman MJ, Zangari M, et al. Inhibitory effects of osteoblasts and increased bone formation on myeloma in novel culture systems and a myelomatous mouse model. Haematologica. 2006;91(2):192-199.
2. Takeuchi K, Abe M, Hiasa M, et al. Tgf-Beta inhibition restores terminal osteoblast differentiation to suppress myeloma growth. PLoS One. 2010;5(3):e9870.
3. Cho YK, Kim SI, Ha KY, Kim YH, Park HY, Min CK. Increased Osteoblastic Activity Suppressed Proliferation of Multiple Myeloma Plasma Cells. Spine (Phila Pa 1976). 2019;44(7):E384-E392.
4. Yaccoby S, Ling W, Zhan F, Walker R, Barlogie B, Shaughnessy JD Jr. Antibody-based inhibition of DKK1 suppresses tumor-induced bone resorption and multiple myeloma growth in vivo. Blood. 2007;109(5):2106-2111.
5. Edwards CM, Edwards JR, Lwin ST, et al. Increasing Wnt signaling in the bone marrow microenvironment inhibits the development of myeloma bone disease and reduces tumor burden in bone in vivo. Blood. 2008;111(5):2833-2842.
6. Shaffer AL, Emre NC, Romesser PB, Staudt LM. IRF4: Immunity. Malignancy! Therapy? Clin Cancer Res. 2009;15(9):2954-2961.
7. Shaffer AL, Emre NC, Lamy L, et al. IRF4 addiction in multiple myeloma. Nature. 2008;454(7201):226-231.
8. Chaudhuri AA, So AY, Sinha N, et al. MicroRNA-125b potentiates macrophage activation. J Immunol. 2011;187(10):5062-5068.
9. Gururajan M, Haga CL, Das S, et al. MicroRNA 125b inhibition of B cell differentiation in germinal centers. Int Immunol. 2010;22(7):583-592.
10. Morelli E, Leone E, Cantafio ME, et al. Selective targeting of IRF4 by synthetic microRNA-125b-5p mimics induces anti-multiple myeloma activity in vitro and in vivo. Leukemia. 2015;29(11):2173-2183.
11. Minamizaki T, Nakao Y, Irie Y, et al. The matrix vesicle cargo miR-125b accumulates in the bone matrix, inhibiting bone resorption in mice. Commun Biol. 2020;3(1):30.
12. Li X, Pennisi A, Yaccoby S. Role of decorin in the antimyeloma effects of osteoblasts. Blood. 2008;112(1):159-168.
13. Ito S, Minamizaki T, Kohno S, et al. Overexpression of miR-125b in Osteoblasts Improves Age-Related Changes in Bone Mass and Quality through Suppression of Osteoclast Formation. Int J Mol Sci. 2021;22(13):6745
14. Wang Y, Zeng G, Jiang Y. The Emerging Roles of miR-125b in Cancers. Cancer Manag Res. 2020;12:1079-1088.

Figure legends

Figure 1. Mature osteoblasts (OBs) suppressed the proliferation of myeloma (MM) cells

(A) MC3T3-E1 preosteoblastic cells were cultured in osteogenic media (25 ng/mL bone morphogenetic protein 2 (BMP-2), 10 mM β-glycerophosphate, and 50 mg/mL ascorbic acid). After confirming the formation of mineralized nodules as indicated at the top, the cells were used as mature OBs. The MM cell lines U266-B1 and NCI-H929 were cultured in triplicate at 1×10^4/mL, 5×10^4/mL, 1×10^5/mL alone (solid line), or co-cultured either with untreated MC3T3-E1 cells (dotted line) or with mature OBs derived from MC3T3-E1 cells (dashed line). (B) IDG-SW3 osteoblastic cells were untreated or cultured in osteogenic media to differentiate into mature OBs as shown in the far left panels. U266-B1 and NCI-H929 cells were cultured in triplicate at 5×10^4/mL alone (solid line) or co-cultured with the mature OBs (dashed line). Viable MM cell numbers were counted at the indicated time points. Percent changes from baseline were compared with those in MM cells cultured alone. The values are mean ± SD (*P < 0.05). (C) U266-B1 and NCI-H929 cells were cultured for 24 hours at 5×10^4/mL alone or cocultured with mature OBs differentiated from MC3T3-E1 cells (left) and IDG-SW3 (right). Protein levels of interferon regulatory factor 4 (IRF4) and MYC were examined by western blotting analysis. Glyceraldehyde-3-phosphate dehydrogenase (GAPDH) was used as a loading control.

Figure 2. Mature OB-derived extracellular vesicles (EVs) induced MM cell death

(A) EVs were isolated from culture supernatants (10 mL) of mature OBs derived from MC3T3-E1 or IDG-SW3 cells using EXORPTION® (Sanyo Chemical) and resuspended in 1 mL (10× concentration). MM cell lines, U266-B1 and NCI-H929, and primary MM cells were cultured at 5.0×10^4 cells/mL in triplicate for 4 days in culture media with or without EVs. The EV solutions were added to the indicated wells to be diluted 1/10 (approximately 10^9 EV particles/mL). Viable cell numbers were counted, and percent changes from the baseline were compared. The values are mean ± SD (*P < 0.05). (B) RNA in EVs (EV-RNA) isolated from mature OBs was labeled using an ExoGlow labeling kit (System Biosciences, LLC). MM cell lines U266-B1 and NCI-H929 were cultured with RNA-labeled EVs from mature OBs for 24 hours. The incorporation of EVs into MM cells was detected by confocal microscopy. The actin filaments and nuclei were stained with Phalloidin (red) and 4',6-diamidino-2-phenylindole (DAPI) (blue), respectively. Scale bars represent 10 μm. (C) The indicated types of cells were incubated in triplicate for 4 days with or without the EVs from mature OBs derived from MC3T3-E1 or IDG-SW3 cells. MC3T3-E1 or IDG-SW3 were seeded at 2×10^5 cells/mL; RAW264.7 cells at 2×10^5 cells/mL; bone marrow stromal cells (BMSC) at 4×10^4 cells/mL; and

peripheral blood mononuclear cells (PBMC) at 1×10^6 cells/mL. Viable cell numbers were counted, and percent changes from the baseline were compared. OB-EV, OB-derived EVs.

Figure 3. EV-mediated transfer of miR-125b suppressed MM cell growth and survival

(A) MC3T3-E1 cells and IDG-SW3 cells with or without OB differentiation were harvested (n=3). OB differentiation was induced after culturing for 10 days in osteogenic media supplemented with 25 ng/m L BMP-2, 10 mM β-glycerophosphate, and 50 mg/mL ascorbic acid. Total RNA was then collected, and miR-125b expression was analyzed by TaqMan MicroRNA Assays (Thermo Fisher Scientific). *U6* served as an endogenous control to normalize each sample. (B) miR-125b levels were analyzed by TaqMan MicroRNA Assays in the indicated cell lines. *U6* served as an endogenous control to normalize each sample. (C) The expression of miR-125b in EVs isolated from human osteoclasts (OC), MM cell lines, U266-B1, and NCI-H929, mouse primary bone marrow stromal cells (BMSC), OB precursors, MC3T3-E1 and IDG-SW3, and mature OBs differentiated from MC3T3-E1 and IDG-SW3 cells. Synthetic *cel-miR-39–3p* was added to EVs from an equal number of cells during RNA extraction, and the levels of *cel-miR-39–3p* were used as exogenous spike-in control for data normalization following TaqMan MicroRNA Assays. (D) The indicated MM cell lines were cultured with or without mature OBs from IDG-SW3. After culturing for 4 days, MM cells were collected and miR-125b expression was analyzed in MM cells by TaqMan MicroRNA Assays. *U6* served as an endogenous control to normalize each sample. Each experiment was repeated three times and data are shown as mean ± SD. $*P < 0.05$. (E) U266-B1 and NCI-H929 cells were cultured for 24 hours with or without of EVs isolated from mature OBs derived from MC3T3-E1 or IDG-SW3 cells. Protein levels of IRF4 and MYC were examined by western blotting analysis. GAPDH was used as a loading control. (F) U266-B1 and NCI-H929 cells were transfected with scrambled (CTL) or a synthetic miR-125b inhibitor using a Human Nucleofector Kit (Lonza). Then, MM cells were cultured in triplicate with or without the EVs isolated from mature OBs derived from MC3T3-E1 or IDG-SW3 cells for 2 days, and viable MM cell numbers were counted. Percent changes from the baseline are shown. $*P < 0.05$. OB-EV, OB-derived EVs.

Figure 1

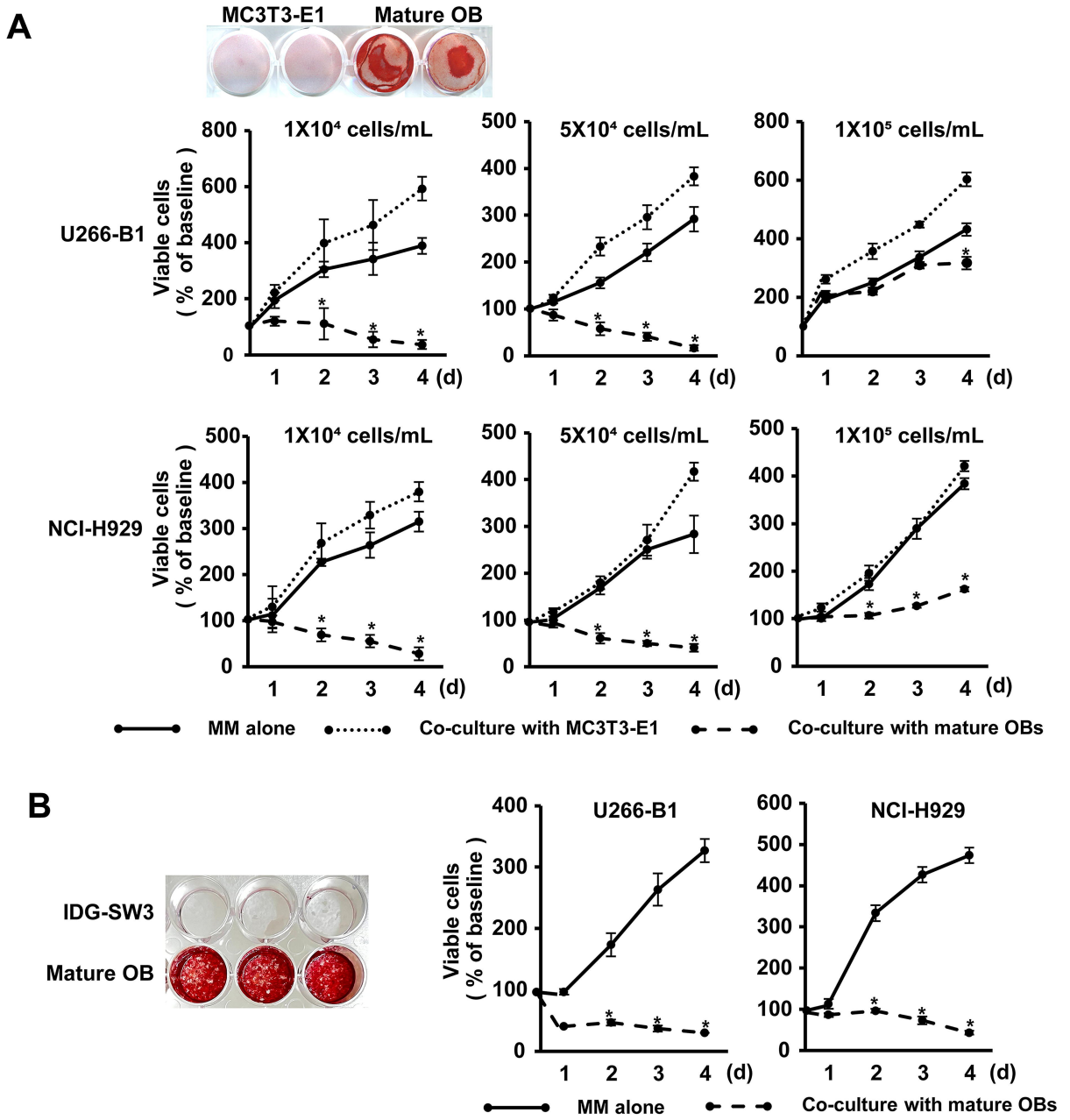
A
MC3T3-E1
Mature OB
U266-B1
NCI-H929
1X10⁴ cells/mL
5X10⁴ cells/mL
1X10⁵ cells/mL
Viable cells (% of baseline)
(d)
MM alone
Co-culture with MC3T3-E1
Co-culture with mature OBs
B
IDG-SW3
Mature OB
U266-B1
NCI-H929
Viable cells (% of baseline)
(d)
MM alone
Co-culture with mature OBs
C
MC3T3-E1
IDG-SW3
Mature OB
(-)
(+)
IRF4
IRF4/GAPDH
1.0
0.3
1.0
0.5
1.0
0.4
1.0
0.4
MYC
MYC/GAPDH
1.0
0
1.0
0.1
1.0
0
1.0
0.1
GAPDH
U266-B1
NCI-H929

Figure 2

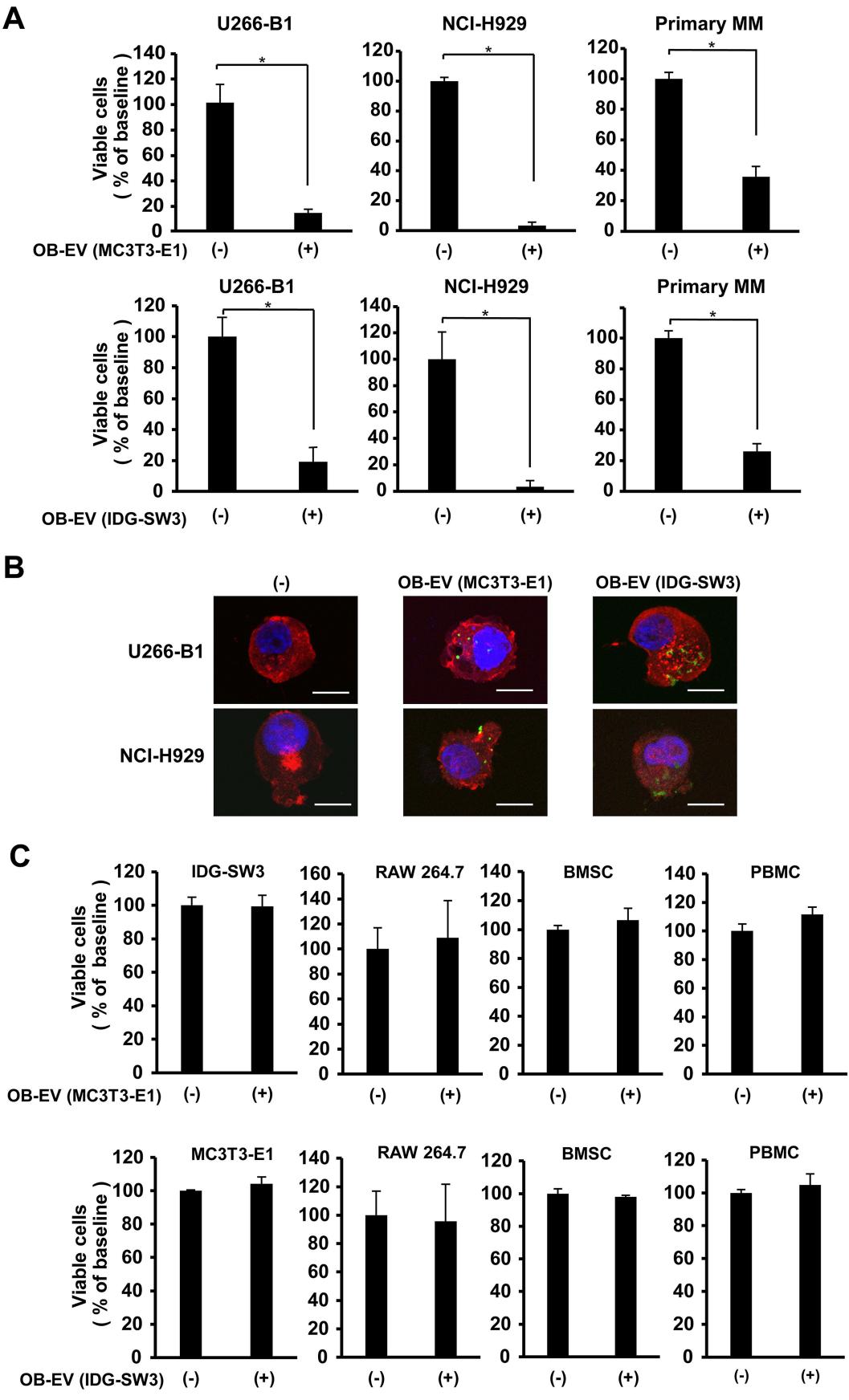
A
U266-B1
NCI-H929
Primary MM
Viable cells (% of baseline)
OB-EV (MC3T3-E1)
OB-EV (IDG-SW3)
(-)
(+)
B
(-)
OB-EV (MC3T3-E1)
OB-EV (IDG-SW3)
U266-B1
NCI-H929
C
IDG-SW3
RAW 264.7
BMSC
PBMC
MC3T3-E1
Viable cells (% of baseline)
OB-EV (MC3T3-E1)
OB-EV (IDG-SW3)

Figure 3

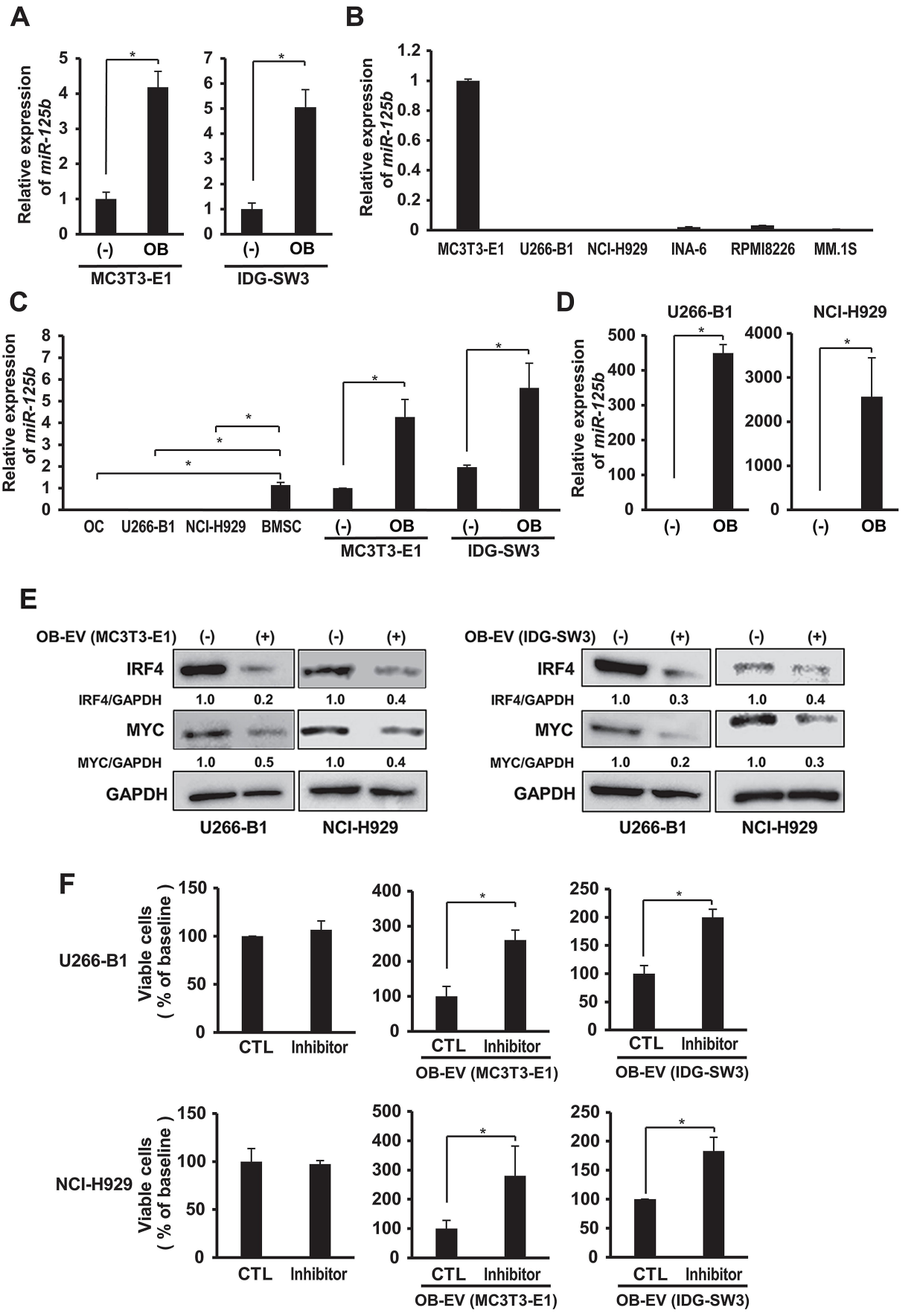
A
Relative expression of miR-125b
(-)
OB
MC3T3-E1
IDG-SW3
B
Relative expression of miR-125b
MC3T3-E1
U266-B1
NCI-H929
INA-6
RPMI8226
MM.1S
C
Relative expression of miR-125b
OC
U266-B1
NCI-H929
BMSC
(-)
OB
MC3T3-E1
IDG-SW3
D
U266-B1
NCI-H929
Relative expression of miR-125b
(-)
OB
E
OB-EV (MC3T3-E1)
OB-EV (IDG-SW3)
IRF4
IRF4/GAPDH
MYC
MYC/GAPDH
GAPDH
U266-B1
NCI-H929
F
U266-B1
NCI-H929
Viable cells (% of baseline)
CTL
Inhibitor
OB-EV (MC3T3-E1)
OB-EV (IDG-SW3)

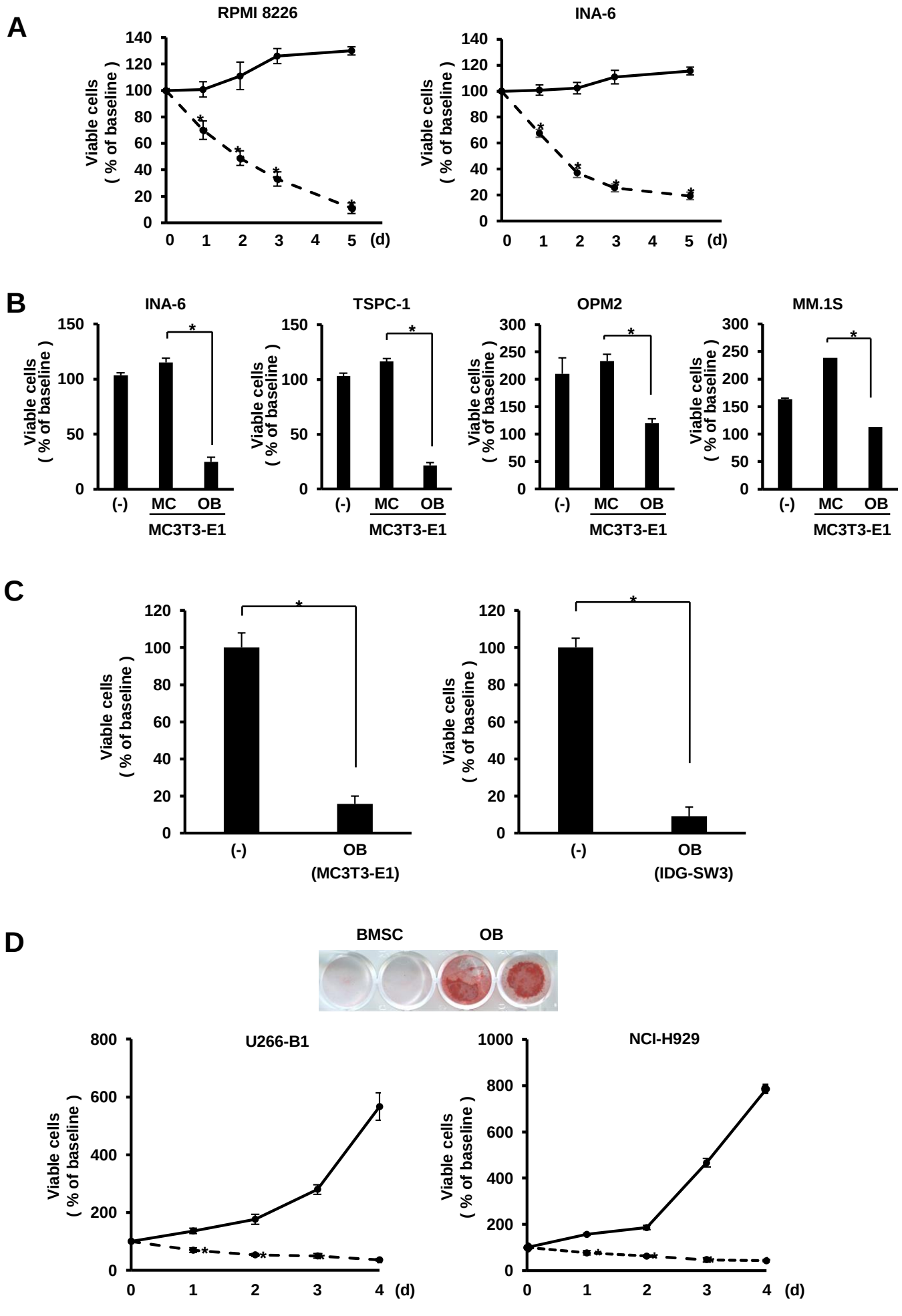

Supplementary Figure 1

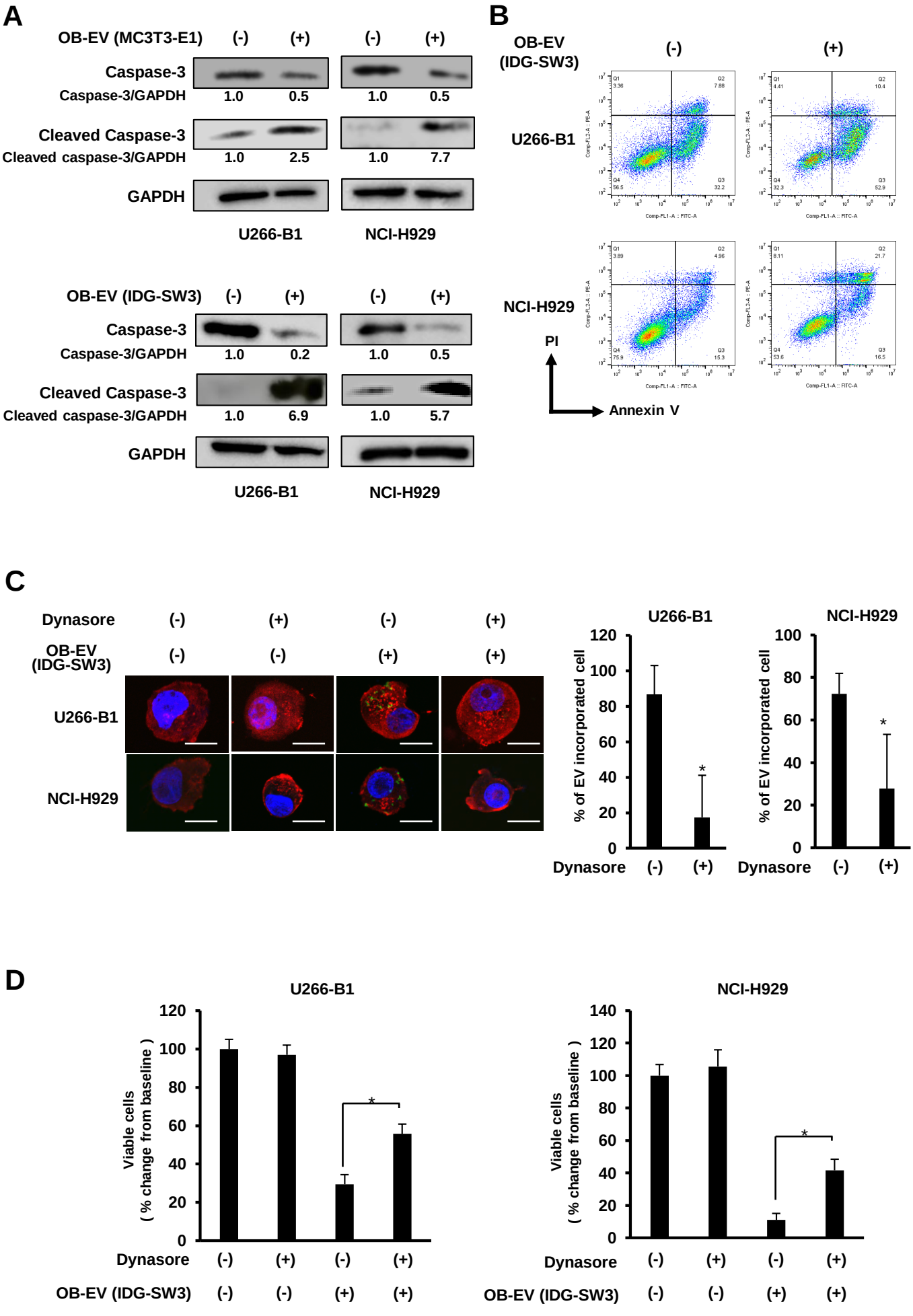

Supplementary Figure 2

A

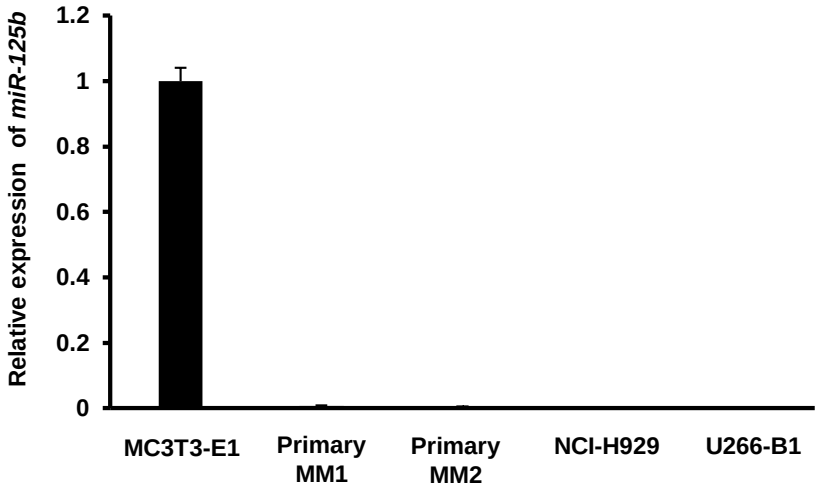

B

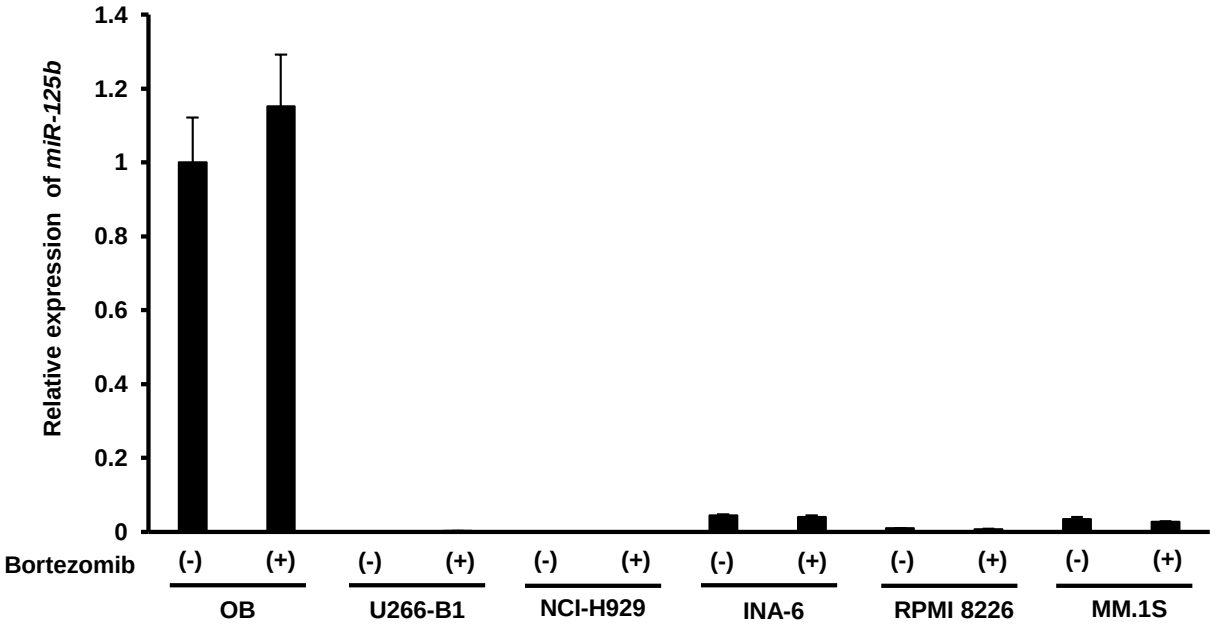

Supplementary Figure 3

Supplementary Figure legends

Supplementary Figure 1

(A) MM cell lines RPMI8226 and INA-6 were cultured in triplicate at 5×10^4/mL alone (solid line) or co-cultured with mature OBs differentiated from MC3T3-E1(dashed line). (B) MM cell lines, INA-6, TSPC-1, OPM-2 and MM1.S, were cultured in triplicate for 2 days at 1×10^5/mL alone (-), or co-cultured either with untreated MC3T3-E1 cells (MC) or with mature OBs derived from MC3T3-E1 cells (OB). (C) MM cells were isolated from patients with MM after receiving informed consent. Primary MM cells were cultured in triplicate for 4 days at 5×10^4/mL alone or co-cultured with mature OBs from MC3T3-E1 or IDG-SW3. Viable MM cell numbers were counted. (D) U266-B1 and NCI-H929 cells were cultured in triplicate at 5×10^4/mL alone (solid line) or co-cultured with mature OBs generated from mouse primary BMSCs (dashed line). Viable MM cell numbers were counted at the indicated time points. Percent changes from the baseline were compared with those in MM cells cultured alone. The values are mean ± SD (*$P < 0.05$).

Supplementary Figure 2

U266-B1 and NCI-H929 cells were cultured for 24 hours in the presence or absence of EVs isolated from mature OBs derived from MC3T3-E1 (OB-EV (MC3T3-E1)) and IDG-SW3 cells (OB-EV (IDG-SW3)). Cell lysates were then collected, and caspase 3 cleavage was analyzed using western blotting analysis (A). GAPDH was used as a loading control. The cells were further analyzed to detect apoptosis by flow cytometry using annexinV and propidium iodide (PI) dual staining (B). (C) MM cells were cultured in the presence or absence of 50 μg/mL Dynasore. After 30 min, RNA-labeled EVs isolated from mature OBs derived from IDG-SW3 cells were added and further cultured for 24 hours. The incorporation of the EVs into MM cells was detected using confocal microscopy. Actin filaments and nuclei were stained with Phalloidin (red) and DAPI (blue), respectively. Representative cell images are shown (left). Scale bars represent 10 μm. The proportion of cells with incorporated EVs in the presence or absence of 50 μg/mL Dynasore was counted under a confocal microscope. The efficiency of the incorporation is shown (right). (D) The indicated MM cell lines were cultured in triplicate in the presence or absence of 50 μg/mL Dynasore. After 30 min, EVs isolated from mature OBs derived from IDG-SW3 cells were added, and MM cells were further cultured for 2 days. Viable cell numbers were counted, and percent changes from the baseline are shown. The values are mean ± SD (*$P < 0.05$).

Supplementary Figure 3

(A) miR-125b levels were analyzed by TaqMan MicroRNA Assays (Thermo Fisher Scientific) in MC3T3-E1, primary MM cells from patients and MM cell lines. (B) mature OBs derived from MC3T3-E1 (OB) and the indicated MM cell lines were cultured with or without pulsatile treatment of bortezomib at 200 nM for 1 hour, which simulates serum pharmacokinetics of bortezomib in patients as previously reported[1]. The cells were then washed to remove bortezomib and further cultured without bortezomib for 24 hours. RNA was collected and miR-125b levels were analyzed by TaqMan MicroRNA Assays. *U6* served as an endogenous control to normalize the data.

Reference

1. Nakaue E, Teramachi J, Tenshin H, et al. Mechanisms of preferential bone formation in myeloma bone lesions by proteasome inhibitors. Int J Hematol. 2023;118(1):88-98.